UCRL-16737

University of California

Ernest O. Lawrence Radiation Laboratory

TWO-WEEK LOAN COPY

This is a Library Circulating Copy which may be borrowed for two weeks. For a personal retention copy, call Tech. Info. Division, Ext. 5545

FIELD ION MICROSCOPE STUDIES OF PLANAR FAULTS

Berkeley, California

DISCLAIMER

This document was prepared as an account of work sponsored by the United States Government. While this document is believed to contain correct information, neither the United States Government nor any agency thereof, nor the Regents of the University of California, nor any of their employees, makes any warranty, express or implied, or assumes any legal responsibility for the accuracy, completeness, or usefulness of any information, apparatus, product, or process disclosed, or represents that its use would not infringe privately owned rights. Reference herein to any specific commercial product, process, or service by its trade name, trademark, manufacturer, or otherwise, does not necessarily constitute or imply its endorsement, recommendation, or favoring by the United States Government or any agency thereof, or the Regents of the University of California. The views and opinions of authors expressed herein do not necessarily state or reflect those of the United States Government or any agency thereof or the Regents of the University of California.

Short course on Field Ion
Spectroscopy - Gainesville, Fla.
March 14-22, 1966
Chapter in book later

UCRL-16737

UNIVERSITY OF CALIFORNIA

Lawrence Radiation Laboratory
Berkeley, California

AEC Contract W-7405-eng-48

FIELD ION MICROSCOPE STUDIES OF PLANAR FAULTS

S. Ranganathan

March 1966

FIELD ION MICROSCOPE STUDIES OF PLANAR FAULTS

S. Ranganathan

ABSTRACT

Field ion microscopy is admirably suited for the investigation of stacking faults of high energies and small widths. The geometry of stacking faults in various metal structures is considered here in relation to the contrast to be expected in field ion micrographs. The conflicting evidence regarding two contrast effects namely streaks and cross-over structures which have been interpreted as stacking faults is reviewed. There is a brief reference to domain boundaries in ordered alloys which are a form of planar faulting.

FIELD ION MICROSCOPE STUDIES OF PLANAR FAULTS

S. Ranganathan

Inorganic Materials Research Division,
Lawrence Radiation Laboratory,
University of California, Berkeley, California

1. Introduction

A perfect dislocation - i.e., its Burger's vector is a unit translation in the lattice - can dissociate into two or more partial dislocations separated by widths of stacking faults. The prerequisite for such a dissociation is that a mechanically stable new configuration should be available. The dissociation reaction leads to a lowering of the elastic energy of the perfect dislocation. This is balanced however by the increase in misfit energy in the plane. Several books on dislocations give excellent treatment of these ideas.[1]

Stacking faults can arise in a material through deformation, aggregation of vacancies (e.g., during quenching) and interstitials (e.g., during irradiation). They affect the x-ray line profiles and lead to broadening as well as peak shifts. However their contribution is not easily isolated from other factors. Thus x-ray line broadening studies[2] have been of limited value. Transmission electron microscope studies[3] have been conspicuously more successful. The faults produce characteristic interference fringes and have been studied extensively in investigations on quenching. The image width of a dislocation is of the order of ~100Å and hence, if the fault width is lower than this, the evidence becomes ambiguous. Also the evidence for stacking faults in b.c.c. metals where the fault energy is expected to be high has been particularly scanty. Therefore field ion microscopy has an important role to play on the observation of stacking faults of small widths and high energies.

The energy of the stacking fault is an important parameter. It affects the mode of deformation - e.g., high energy stacking fault materials permit easy cross-slip. It can also affect stress-corrosion. Methods of varying reliability exist for the evaluation of the energy. If field ion microscopic observations can shed light on this aspect, it should be welcome.

In this article we shall be solely concerned with the geometry of the stacking fault and its probable contrast in field ion micrographs. We shall begin with a consideration of stacking fault geometry in f.c.c. and b.c.c. structures. At one time streaks observed in field ion micrographs were interpreted as stacking faults.[4] The question of streak contrast[5] receives full discussion here. Ryan and Suiter[6] have interpreted a cross-over effect in tungsten micrographs as stacking faults on {111} planes. This contrast effect can also be interpreted as arising from nodes in a dislocation network.[7] The last two sections deal with two structurally simple instances - stacking faults in the h.c.p. structure and domain boundaries in ordered alloys.

2. Stacking Faults in the Face Centered Cubic Lattice[1]

The face centered cubic structure can be considered to be made up of the stacking sequence ABC ABC based on (111) planes. There are three types of partial dislocations associated with faults in this stacking sequence: a Shockley partial and two Frank partials. In the case of the Shockley partial, the Burger's vector lies in the plane of the fault: for a Frank partial the Burger's vector is not parallel to the fault and hence it is sessile.

Figure 1a illustrates a Shockley partial with Burger's vector $\frac{1}{6}[1\bar{2}1]$ on the (111) plane. The figure is for the dislocation in edge orientation.

The partial can arise from the following dissociation.

$$\frac{a}{2}[\bar{1}10] \rightarrow \frac{a}{6}[\bar{2}11] + \frac{a}{6}[\bar{1}2\bar{1}]$$

Figure 1b illustrates a Frank partial with Burger's vector - $\frac{1}{3}$ [111]. Note that the partial is sessile. Also the fault is the same as in Fig. 1a.

Evidence for the existence of these partial dislocations and stacking faults rests on a firm experimental basis. Furthermore, interactions among the partials leading to the formation of Lomer-Cottrell locks and stacking fault tetrahedra have been observed.[3]

3. Stacking Faults in the Bodey Centered Cubic Lattice[1]

As detailed transmission electron microscope studies of b.c.c. refractory metals have been lacking until recently, there is a great deal of confusion with regard to the presence of stacking faults in the b.c.c. lattice. Hirschhorn[8] has given an excellent summary of possible dislocation dissociations on {112}, {011} and {310} planes.

The b.c.c. lattice can be considered to be built up of an ordered sequence of six planes ---ABCDEFAB--- based on {112}. Faults in this stacking sequence can arise from a dissociation of dislocations. Two reactions have received detailed attention.

$$\frac{a}{2}[111] \rightarrow \frac{a}{3}[112] + \frac{a}{6}[11\bar{1}] \qquad (1)$$

The first partial is pure edge and sessile; and the second partial is pure screw and glissile. As $[11\bar{1}]$ is the line of intersection of three {112} planes, the second partial can glide out of the original plane of dissociation and create a dihedral stacking fault. It should be noted that there is no energy change on the Burger's vector square

energy criterion.

$$\frac{a}{2}[11\bar{1}] \rightarrow \frac{a}{6}[11\bar{1}] + \frac{a}{3}[11\bar{1}] \qquad (2)$$

The two partials are pure screw and can once again glide out of the original slip plane. Sleeswyk[9] has considered an interesting variant of this reaction. If the original dislocation is pure screw, further dissociation into three partials can occur.

$$\frac{a}{2}[11\bar{1}] \rightarrow \frac{a}{6}[11\bar{1}] + \frac{a}{3}[11\bar{1}] + \frac{a}{6}[11\bar{1}]. \qquad (2a)$$

This results in a twofold symmetrical configuration of the three partials with one in the center and two at equidistant positions on different {112} planes.

Other types of dissociation on (112) planes have also been considered.

$$\frac{a}{2}[111] \rightarrow \frac{a}{6}[11\bar{1}] + \frac{a}{6}[133] + \frac{a}{6}[1\bar{1}1] \qquad (3)$$

$$\frac{a}{2}[111] \rightarrow \frac{a}{6}[11\bar{1}] + \frac{a}{6}[113] + \frac{a}{6}[111] \qquad (4)$$

Faults on other planes [e.g., (011) by Cohen et al.,[10] (310) by Segall[11]] have also been theoretically treated. Possible dissociations have been listed here in detail so that an attempt could be made to consider the contrast from stacking faults arising through these reactions from a theoretical view point. There are few experimental observations of stacking faults in b.c.c. metals. Hirsch and Segall[12] found that the faults were on {310} planes in niobium. Nakayama et al.[13] have observed stacking faults in tungsten quenched from above 2000°C and derived a value of $\gamma_{S.F.} = 14.5$ ergs/cm^2 for impure tungsten. The work on alloys is slightly more definitive. Votava[14] has noted the existence of stacking faults on {112}planes in foils of molybdenum-35% rhenium.

4. Contrast To Be Expected From Partial Dislocations and Stacking Faults

Moore[15] has tried to account for the pattern in a field ion micrograph on the basis of pure geometry. A sphere was imagined to cut an infinitely extended crystal and all the material outside the sphere removed. A computer was used to plot in orthographic projection the positions of atoms that are within a certain distance from the surface of the sphere. The resulting pattern had a striking resemblance to the field ion image. Moore presented a paper at the 11th Field Emission Symposium in Cambridge (1964) extending this approach to alloys and showed how the flexibility and the speed of the computer aided the choice of various possibilities leading to an image from the alloy. This approach holds great promise and is capable of being extended to the surfaces of imperfect crystals. This has not been done up to the time of writing this review. Hence a qualitative approach will be adopted in the subsequent discussions.

When a perfect dislocation of Burger's vector $\bar{b}$ intersects the crystal surface on a particular net plane ($\bar{g}$ is the plane normal) a spiral will arise so long as $\bar{g} \cdot \bar{b} \neq 0$. This is similar to the visibility criterion in electron microscopy. The spiral is due to the component of the Burger's vector normal to the plane. If the component is equal to multiple interplanar spacing, a series of interleaved helicoids are expected. To follow Frank's terminology,[16] unlike the ideal crystal of n layers, the dislocated crystal consists of one layer only in the form of a helicoid. When the dislocation is of multiple strength, we have a crystal of several interleaved helicoidal lyaers. When it contains a number of dislocations, it consists of a number (possibly one) of similar interleaved 'expanded Riemann surfaces.'

Such information can be used for the determination of Burger's vector of a dislocation from field ion micrographs.[17]

The extension of these concepts to partial dislocations is not easy. A partial dislocation intersecting a close packed plane will still be invisible if $\bar{g} \cdot \bar{b}_p = 0$ (for an exception in rhenium see section 7). Thus an extended dislocation on the (111) plane can be missed on the net planes of (111). However, a stacking fault on any one of $(\bar{1}11)$, $(1\bar{1}1)$ $(11\bar{1})$ will be visible on the (111) plane rings. In electron microscopy if $\bar{g} \cdot \bar{b}_p = \pm \frac{1}{3}$ then also the partial dislocation is invisible or gives very weak contrast.[3] It will be interesting to apply this rule to contrast in field ion microscopy.

The foregoing considerations entirely ignore the real situation in a specimen being studied by field ion microscopy. The dislocations are emerging at the surface. The surface is under an electrostatic stress. The specimen is finally subjected to the process of field evaporation. These three factors should be remembered in interpreting the image of a defect. The last factor has been considered by Brandon[18] in some detail. The surface section taken by field evaporation does not remain smooth in the case of a defect lattice. The variations in binding energy and lattice geometry at a lattice defect always result in some modification of the surface section. The problem is somewhat analogous to that experienced with chemical etching: the preferential removal of some atoms at the core of the defect can lead to field enhancement effects on neighboring atoms so that a field evaporation "etch pit" is formed at the defect. The successful interpretation of the field-ion image thus depends very much on the correct estimate of the extent of cooperative evaporation.

5. Streak Contrast

Bright streaks are frequently observed in the field-ion images of specimens which have been subjected to certain treatments. There was considerable discussion of the possible causes for these image imperfections at the 11th Field Emission Symposium in Cambridge. A subsequent paper by Ranganathan et al[5] catalogued the different types of streaks and went some way towards interpreting their origins. The following summary draws heavily on this paper.

5.1 The Case of Tungsten-Rhenium Alloys

Ralph and Brandon[4] came across the first reproducible observations of image streaking in their study of the tungsten-rhenium system. Small streaks were found in deformed tungsten-rhenium alloys (Fig. 2) which were interpreted as being due to the step produced where a stacking fault or a {112} plane intersects the crystal surface (Fig. 3). Preferential evaporation of atoms situated on the step was not thought likely since the atoms have the same coordination number and binding energy (though with a different disposition of neighbours) as other atoms giving rise to image points. Atoms on the step should however give bright images due to field enhancement and focusing of field contours over the ridge formed by the fault.

Further consideration shows that a strong field enhancement factor does not exist on (110) planes. The intersection of two faulted planes - the diagram corresponds to the deformation fault with the stacking sequence AB CD <u>CD</u> EFA - merely produces a kink on the (110) plane. While the atoms at the kink may give slightly enhanced intensity, the effect will not be the same as a step normal to the (110) plane. Such a step exists on planes inclined to (110) e.g., $(11\bar{2})$. Also this deformation fault corresponds to

the first dissociation reaction described in Section 3 where a sessile $\frac{a}{3}$ [112] dislocation forms the boundary for two fault planes. When through field evaporation a number of atom layers have been taken off, most streaks disappear. They do this in a gradual fashion and no special effect that will indicate the existence of a sessile dislocation has been seen.

5.2 Streaks Where an Unambiguous Identification is Possible:
a) Image Superposition b) Interfaces

Image superposition can lead to streaking. Figure 4 whows streaking arising from image superposition round the jagged edge of a surface crater in tungsten.

Streaking at grain boundaries is fairly common. The presence of a grain boundary is readily detectable in the field-ion image because planes appear to be rotated out of their normal positions on the image about the axis of misorientation. Thus there is little likelihood of streaks due to grain boundaries being confused with those generated by other mechanisms. Both electronic and geometrical factors can lead to such streaking. Figure 5 shows a streak arising from a geometrical step on the surface at a grain boundary in tungsten. Holland[19] has shown that localized electronic states exist in the vicinity of planar defects including grain boundaries. Such electronic effects could well give rise to preferential ionization along the line of the boundary. Grain boundaries are also observed occasionally with a dark band (Brandon et al[20]) lying along the boundary. These effects could be connected.

5.3 Characteristics of Streaks in Asymmetric Tips - The Most Interesting Case

Asymmetric tips show some of the most drastic cases of streaking. The asymmetry of the tip is very striking. The radii from the central (110) to each of two neighbouring {112} poles often differ by a factor of 3. Sometimes the asymmetry is so pronounced that a measurement of the radii from the number of rings is not possible. Estimation from the appearance of high index planes would lead to factors as high as ten.

There is a definite crystallographic nature to the asymmetry of the specimens under consideration. The specimens have an elliptical cross-section and in general fall into two categories as illustrated in Fig. 9. Tungsten has a preferred orientation which results in the tip axis invariably being [110]. In one type of asymmetry the major and minor axes of the ellipse are $[\bar{1}12]$ and $[1\bar{1}1]$ respectively. In the second less common type of asymmetry the major and minor axes can be specified as $[\bar{1}10]$ and [001] respectively. Since in both cases the streaks lie perpendicular to the major axis of the ellipse and also run parallel to the axis of the wire (as can be demonstrated by field evaporation) the planes on which the streaks lie can be specified accurately.

It is found that streaks lie on {112} or {110} planes, and it is significant that these are the slip planes for the b.c.c. system. Examples of streaks lying on {112} and {110} planes are shown in Figs. 6 and 7 respectively.

In the case of f.c.c. metals (e.g., platinum and iridium) asymmetry and associated streaking have also been observed. Although the body of evidence is smaller in this case, the streaks have always been found to lie on {110} planes (Fig. 8). The {110} planes in f.c.c. metals play no

special part in deformation and the occurrence of streaks on these planes remains to be explained satisfactorily.

As Müller[21] has observed, field evaporation of an asymmetric tip does not produce a completely symmetric tip, but the degree of asymmetry is reduced. Similarly, when a tip containing streaks is field-evaporated, the streaks and the associated distortion persist, although a few streaks may be removed. As a general rule, the number of streaks decreases with an increase in radius, strongly suggesting that the disturbance is confined to the top few hundred atom layers of the tip. An interesting observation is that streaks tend to split into two halves when the radius has been increased by field evaporation. Examples of such splitting are visible in Fig. 6.

5.4 Distinction From Slip Bands

Slip bands are easily distinguished from streaks. The shear stress component of the electric field in the case of an asymmetric tip can lead to slip (Fig. 10). A corrugated surface produced by slip should assume a smooth shape after field evaporation and this is at variance with the persistence of streaks. The crystallography of streaks in f.c.c. metals cannot be explained as well.

5.5 Contrast Theory

Basically streaks appear to be a planar type of imperfection. They are a gross structural feature in field ion micrographs and are seldom clearly resolved. The most likely explanation is that streaks are a structural feature introduced during the process of specimen preparation. While both the electropolishing process and the field necessary for imaging can lead to the deformation of the specimen, the former is more

important. With the use of a two-layer electrolyte, the detachment of the bottom portion of the wire at the end of the polishing process could lead to severe stresses and deformation of the metal. A rough estimate shows that the stress can reach values as high as 10^{10} dynes cm^{-2}. The asymmetry of the wedge shaped specimen is again a function of the polishing process. As conditions of polishing vary from specimen to specimen, the random observation of streaks with no correlation with the state of the metal is not surprising. The effect of the imaging field on an asymmetric specimen is two-fold: the shear components of the field stress may lead to the deformation of the specimen and the field variations over the elliptical surface can lead to a variable magnification in the image.

6. The Cross-Over Structure in Tungsten

A planar defect structure[6] which has received considerable attention and can be interpreted with some confidence is the so-called "cross-over structure" in tungsten (Fig. 11). It is easily recognized and well-defined. There is no extra half plane corresponding to the (011) planes. These net planes are seen to be drawn inwards. Similar micrographs have appeared in earlier work on tungsten by Ranganathan[22] and on platinum by Müller.[23] Ryan and Suiter[6] have added the further remarkable observation that the effect disappeared over a hundred layers and then reappeared again in the same place. Their observations are described below.

From many observations it has been found that these defects show the following characteristics: their maximum extent in the $[2\bar{1}1]$ direction is generally less than 30Å, the lattice disturbance is usually evident for distances in the [011] direction of the order of a hundred angstroms and the spacing in the [011] direction between disturbed regions is some

200-400 Å. Sometimes the defect has been observed on a grain boundary (Fig. 12). These defects have been found in drawn wires as well as wires that have been heated to 700-1300°C while under stresses ranging up to fracture stress. However the number of observations is not sufficiently large to enable their origin to be associated with any particular conditions of stress or temperature.

Ryan and Suiter interpret the cross-over structure in terms of the diagram (Fig. 13a). They believe that it arises from an extended dislocation on the (111) plane. The dislocation reaction is thought to be similar to that proposed by Cohen et al,[10]

$$\frac{a}{2}[\bar{1}1\bar{1}] \rightarrow \frac{a}{8}[\bar{1}0\bar{1}] + \frac{a}{4}[\bar{1}2\bar{1}] + \frac{a}{8}[\bar{1}0\bar{1}]$$

If the dislocation extends by the movement of one of the $\frac{a}{8}[10\bar{1}]$ partials, faulting will occur on the $(11\bar{1})$ plane and the distrubance of the field ion micrograph can arise from a number of effects due to the partial dislocations, the stacking fault and the field evaporation process. The three partial dislocations are all of mixed character so that instead of having closed rings for the edges of the (011) planes in the vicinity of the extended dislocations a type of spiral will occur starting and finishing on the ends of the stacking fault and passing through each partial dislocation. The shear displacement across the stacking fault will produce a distrubance in the image if there is an appreciable component normal to the surface being examined. The extent of these effects may be exaggerated by the phenomenon of field evaporation. While the fault energy on a {111} plane should be high, impurities in the specimen could have led to a segregation to the stacking fault and a consequent lowering in its energy.

The author[7] has made similar observations of cross-over structures in tungsten (and iridium). The observational details generally confirm those of Ryan and Suiter. It was further observed that the effect could appear in a different place. Also in between such effects, there was a residual contrast: in a particular case a single (011) plane was found to exhibit a closure failure.

In the model proposed by Ryan and Suiter, an edge dislocation lying on a {112} plane prefers to dissociate on a {110} plane and then the partials spread out on a {111} plane. This sequence appears highly improbable on energy considerations. Besides, there is no evidence for the presence of the partial dislocations with the given Burgers vectors. The reason for preferring the particular mode of dislocation dissociation appears to be that two of the partial dislocations could move on a {111} plane - the fault plane demanded by observation. The author has observed similar structures on both {111} and {100} planes. Hence a more general explanation appeared desirable.

The regular and repeated occurrence of the defect seems to favour an interpretation on the basis of a dislocation network (Fig. 13b). In the case of tungsten, such a network can be formed by the reaction

$$\frac{a}{2}[111] + \frac{a}{2}[\bar{1}1\bar{1}] \rightarrow a[010]$$

The locking in of the dislocations might explain their stability in the presence of the field. In this interpretation, the disturbed structure would correspond to the asymmetrical three-fold node formed by this reaction. Nets of this type observed in iron have been analyzed by Carrington et al.[24] In tungsten, also, such networks have been noted and a feature of many of these networks is the close spacing (~ 100Å) of the dislocations (F. O. Jones[25]).

On the basis of the network theory, away from the node, one should expect contrast from three dislocations with Burgers vectors $(\frac{a}{2})$ [111], $\frac{a}{2}$ $[\bar{1}1\bar{1}]$ and a[010]. When these dislocations intersect the (011) planes $(\frac{a}{2})$ [111] and a[010] dislocations should give rise to spirals on the (011) planes, while the $(\frac{a}{2})$ $[\bar{1}1\bar{1}]$ dislocation will not give rise to a spiral regardless of its edge or screw components. The author believes that it is possible to associate the closure failure of the (011) plane with this dislocation. The spirals from the other two dislocations were not observed. Further observations are necessary to check whether these dislocations with the associated spirals occur. These observations are awaited with interest.

7. Stacking Faults in H.C.P. Metals

The normal stacking sequence for h.c.p. metals is ABAB.... A fault involves three or more planes in the ABC order characteristic of f.c.c. All stacking faults in hexagonal crystals are on basal planes; so any given partial dislocation is confined to a basal plane.

Müller[26] has studied Re, Zr, Co, Zn, and Be. However only rhenium has received detailed attention. The basal plane has been observed by using single crystals grown in the c direction. Müller observed that net plane edges near the (0001) plane alternated in intensity due to the stacking sequence. Hence a stacking fault can be identified by its disturbance of this alternating effect. (The intensity alteration is spectacular and a complete explanation is not yet available.)

Müller[27] has also published hydrogen ion images of cobalt. Extensive studies of this metal should be of great interest as cobalt exhibits a phase transformation from h.c.p. to f.c.c. and has a low stacking fault energy.[28]

8. Domain Boundaries

The field ion micrographs from ordered alloys resemble those of metals in regularity and allow detailed interpretation.[29,30] In an ordered alloy domain boundaries are expected whenever two domains which are out of phase meet. The domain boundary is a kind of stacking fault in the superlattice and may end on a lattice dislocation of the disordered structure which becomes a partial dislocation of the superlattice. Southworth and Ralph[31] have presented examples of domain boundaries in cobalt-platinum. Figure 14 shows a translational domain boundary crossing the (001) region). Its interface plane is (010) which provides the lowest energy condition. The boundary is identified as the antiphase structure produces a characteristic bright spot/vacant site contrast feature at the boundary. If adjacent domains choose different cube axes of the parent grain for their (tetragonal) c axis, then a rotational domain boundary results when the domains meet. The paper by Southworth and Ralph[30] reports an example where the interface was lying on a {111} plane.

7. Acknowledgments

The author would like to thank Mr. K. M. Bowkett, Dr. D. G. Brandon, Dr. B. Ralph, Dr. H. F. Ryan, Dr. H. N. Southworth, and Dr. J. Suiter for the supply of illustrative material for this review. He is grateful to Professor G. Thomas for encouragement and helpful discussions and the United States Atomic Energy Commission for financial support.

REFERENCES

1. A. H. Cottrell, Dislocations and Plastic Flow in Crystals, (Oxford University Press, London, 1953); W. T. Read, Dislocations in Crystals (McGraw-Hill Book Company, Inc., New York, 1953); J. Friedel, Dislocations, (Pergamon Press, London, 1964).

2. B. E. Warren, Progr. Met. Phys., 8, 147 (1959).

3. G. Thomas, Transmission Electron Microscopy of Metals (John Wiley and Sons, Inc., New York, 1962).

4. B. Ralph and D. G. Brandon, Phil. Mag., 8, 919 (1963).

5. S. Ranganathan, K. M. Bowkett, J. Hren and B. Ralph, Phil. Mag., 12, 841 (1965).

6. H. F. Ryan and J. Suiter, J. Less Comm. Metals, 9, 258 (1965).

7. S. Ranganathan, J. Less Comm. Metals (in press).

8. J. S. Hirschhorn, J. Less Comm. Metals, 5, 493 (1963).

9. A. W. Sleeswyk, Phil. Mag., 8, 1467 (1963).

10. J. B. Cohen, R. Hinton, K. Lay and S. Sass, Acta Met., 10, 894 (1962).

11. R. L. Segall, Acta Met., 9, 975 (1961).

12. P. B. Hirsch and R. W. Segall, Substructure and Mechanical Properties of Crystals, WADD TR-61-181, 1961.

13. Y. Nakayama, S. Weissman, and T. Imura, in Imperfections in Crystals, (Interscience, New York, 1961) p.573.

14. E. Votava, Acta Met., 10, 745 (1962).

15. A. J. W. Moore, J. Phys. Chem. Solids, 23, 907 (1962).

16. F. C. Frank, Advances in Physics, 1, 91-109 (1952).

17. S. Ranganathan, (in preparation).

18. D. G. Brandon, AIME Conference on High Temperature and High Resolution Microscopy, Chicago, 1964.

19. B. W. Holland, Phil. Mag., 8, 87 (1963).

20. D. G. Brandon, B. Ralph, S. Ranganathan, and M. Wald, Acta Met., 12, 813 (1964).

21. E. W. Müller, Acta Met., 6, 620 (1958).

22. S. Ranganathan, Third European Regional Conference on Electron Microscopy, Prague, 1964, p. 265.

23. E. W. Müller, Fourth International Conference on Electron Microscopy, Berlin, 1, 820 (1958) (Springer Verlag).

24. W. Carrington, K. F. Hale and D. McLean, Proc. Roy. Soc., A259, 203 (1960).

25. F. O. Jones, J. Less Comm. Metals, 2, 163 (1960).

26. E. W. Müller, Third European Regional Conference on Electron Microscopy, Prague, 1964, p. 161.

27. E. W. Müller, in Direct Observations of Imperfections in Crystals, (Interscience, New York, 1961), p. 77.

28. T. R. Anantharaman and J. W. Christian, Acta Cryst., 9, 479 (1956).

29. E. W. Müller, Bull. Am. Phys. Soc., 7, 27, (1962).

30. B. Ralph and D. G. Brandon, Journees Int. Des Applications Du Cobalt, (9-11 June, 1964) p. 76.

31. H. N. Southworth and B. Ralph, Phil. Mag. (Submitted for publication).

FIGURE CAPTIONS

Fig. 1a Illustration of a Shockley Partial with Burgers vector - $\frac{a}{6}[1\bar{2}1]$ - (in edge orientation) with associated stacking fault in face-centered cubic. The plane of the figure is $(\bar{1}01)$ and the dislocation runs normal to this plane. Only one plane has been shown.

Fig. 1b A Frank partial with associated stacking fault in face-centered cubic.

Fig. 2 Tungsten - 5% rhenium showing bright lines (Ralph and Brandon[4]).

Fig. 3 $(1\bar{1}0)$ projection of a b.c.c. lattice containing a stacking fault and showing that a step is produced on the surface (Ralph and Brandon[4]).

Fig. 4 Streaks arising from image superposition round the jagged edges of a surface crater in tungsten (Courtesy K. M. Bowkett) Ref. 5.

Fig. 5 Streak arising from a geometrical step on the surface at a grain boundary in tungsten, Ref. 5.

Fig. 6 Streaks lying on {112} planes in tungsten, Ref. 5.

Fig. 7 Cold-worked neutron-irradiated tungsten. The streaks lie on {110} planes. (Courtesy K. M. Bowkett) Ref. 5.

Fig. 8 Asymmetric iridium specimen. Streaks lie on {110} planes.

Fig. 9 Stereograms illustrating the crystallography of the two types of elliptical asymmetry found in tungsten (Ranganathan et al[5]).

Fig. 10 Slip bands in platinum.

Fig. 11 Field ion micrograph of characteristic defect structure in tungsten.

Fig. 12 The defect structure at a boundary in tungsten. The sequence brings out the appearance and disappearance of the structure. (Courtesy H. F. Ryan and J. Suiter[6]).

Fig. 13a Schematic representation of proposed dislocation arrangement. (H. F. Ryan and J. Suiter[6]).

Fig. 13b Proposed explanation on the basis of a dislocation network (S. Ranganathan[7]).

Fig. 14 A domain boundary in ordered cobalt-platinum (Courtesy H. N. Southworth and B. Ralph[31]).

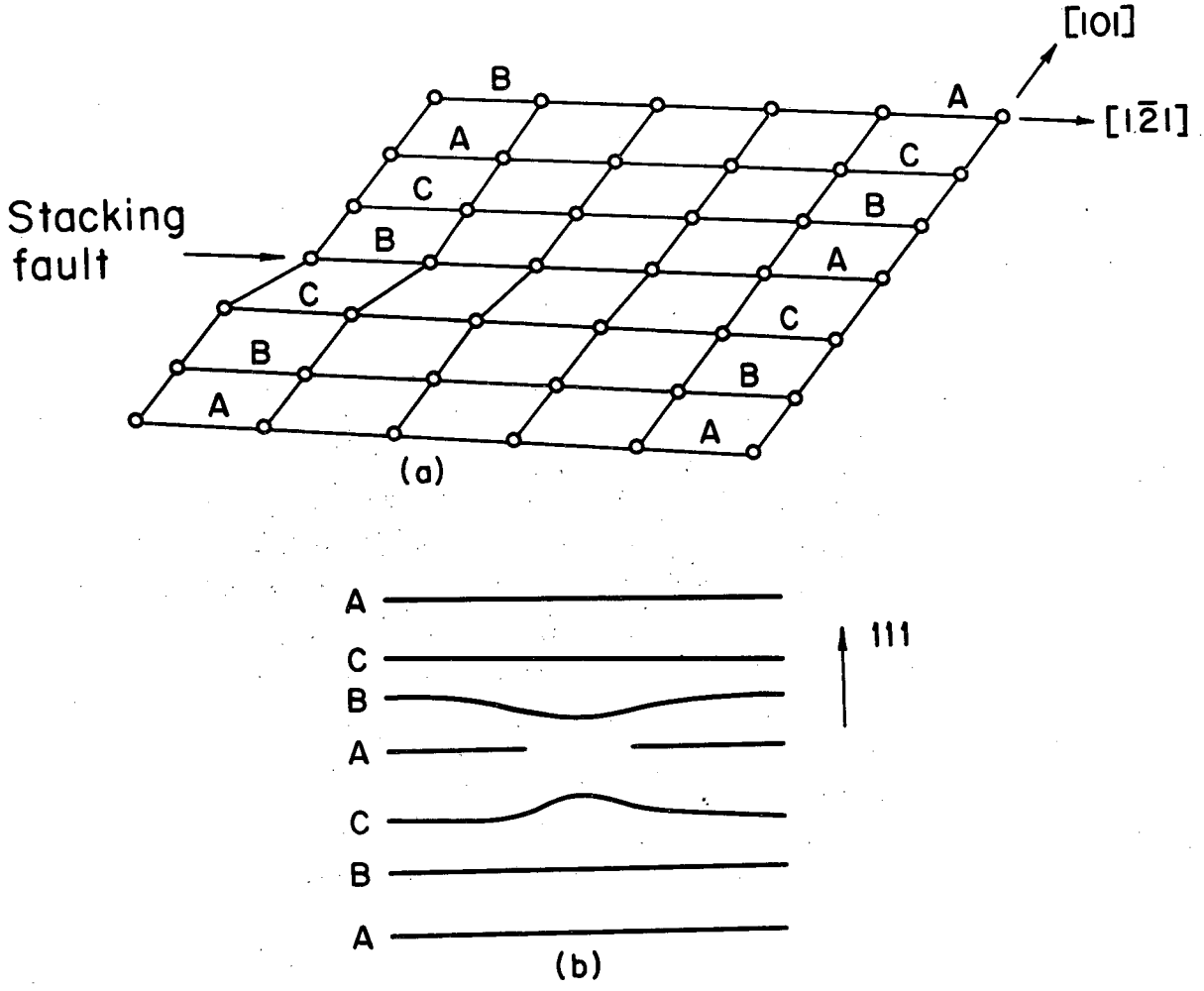

MUB-9692

Fig. 1

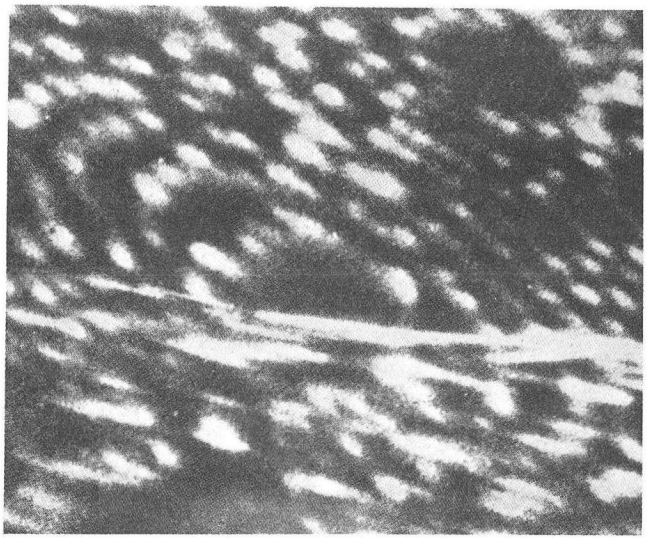

ZN-5398

Fig. 2

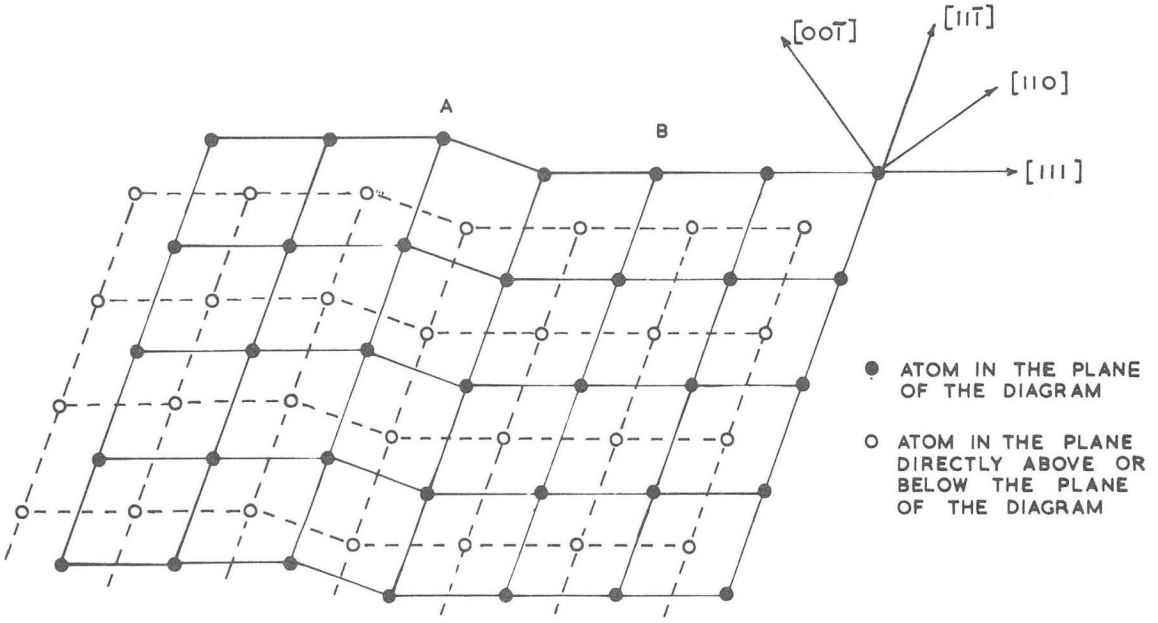

MUB-9688

Fig. 3

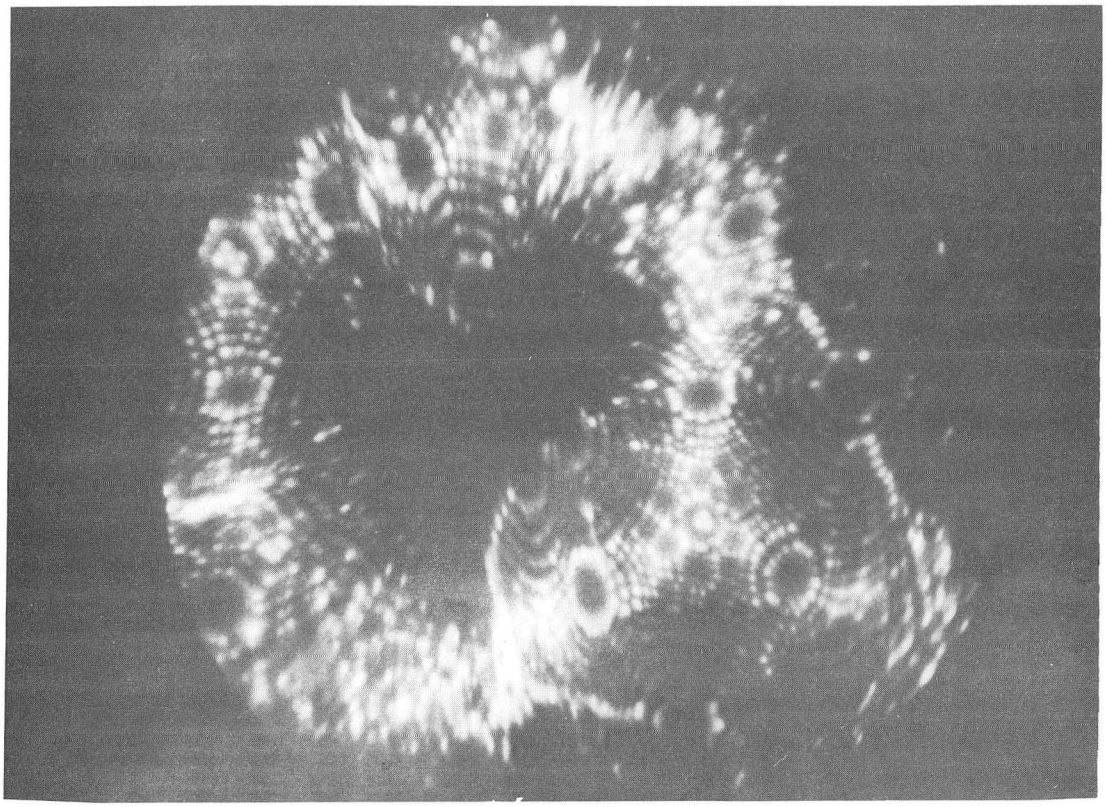

ZN-5291

Fig. 4

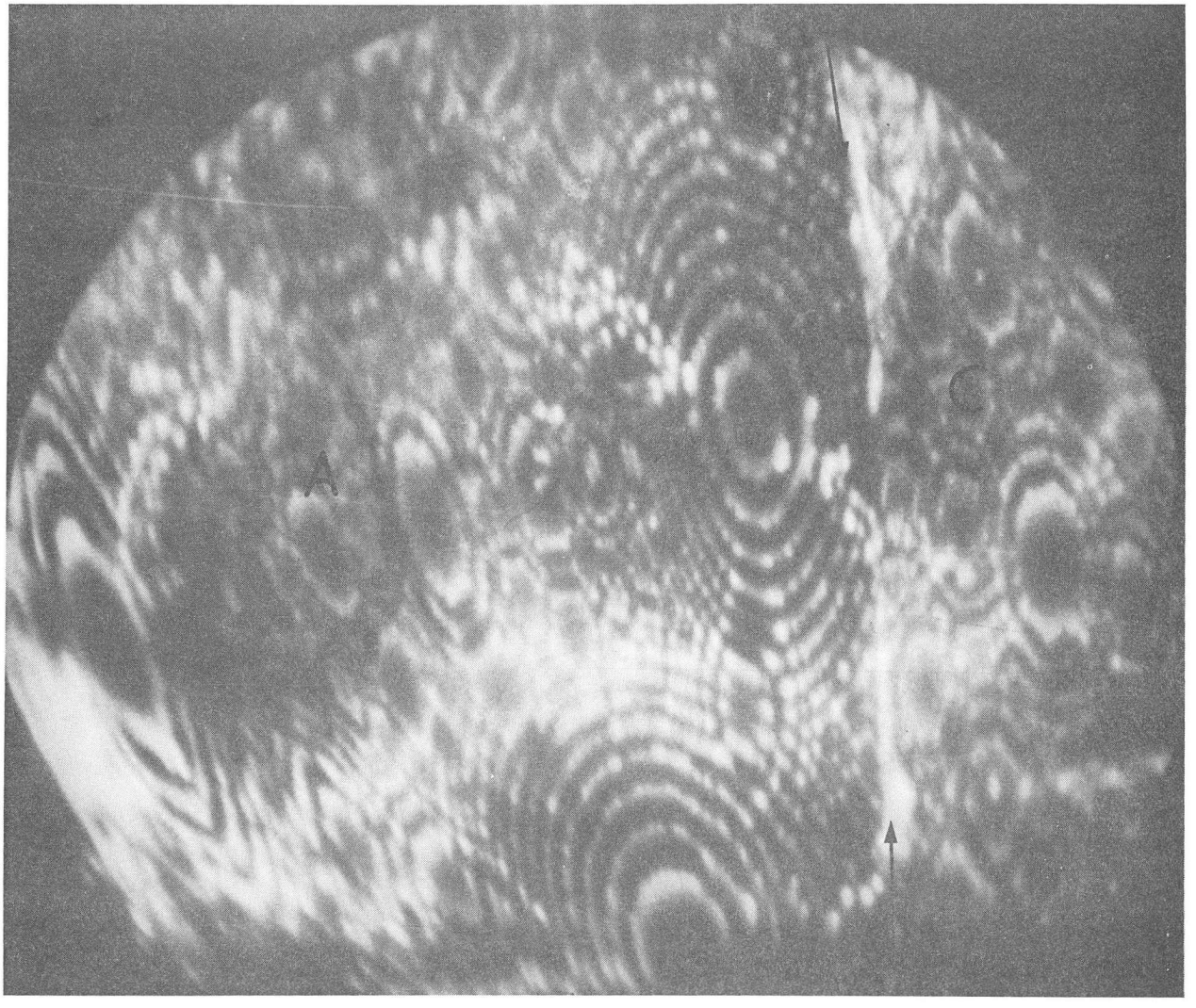

ZN-5390

Fig. 5

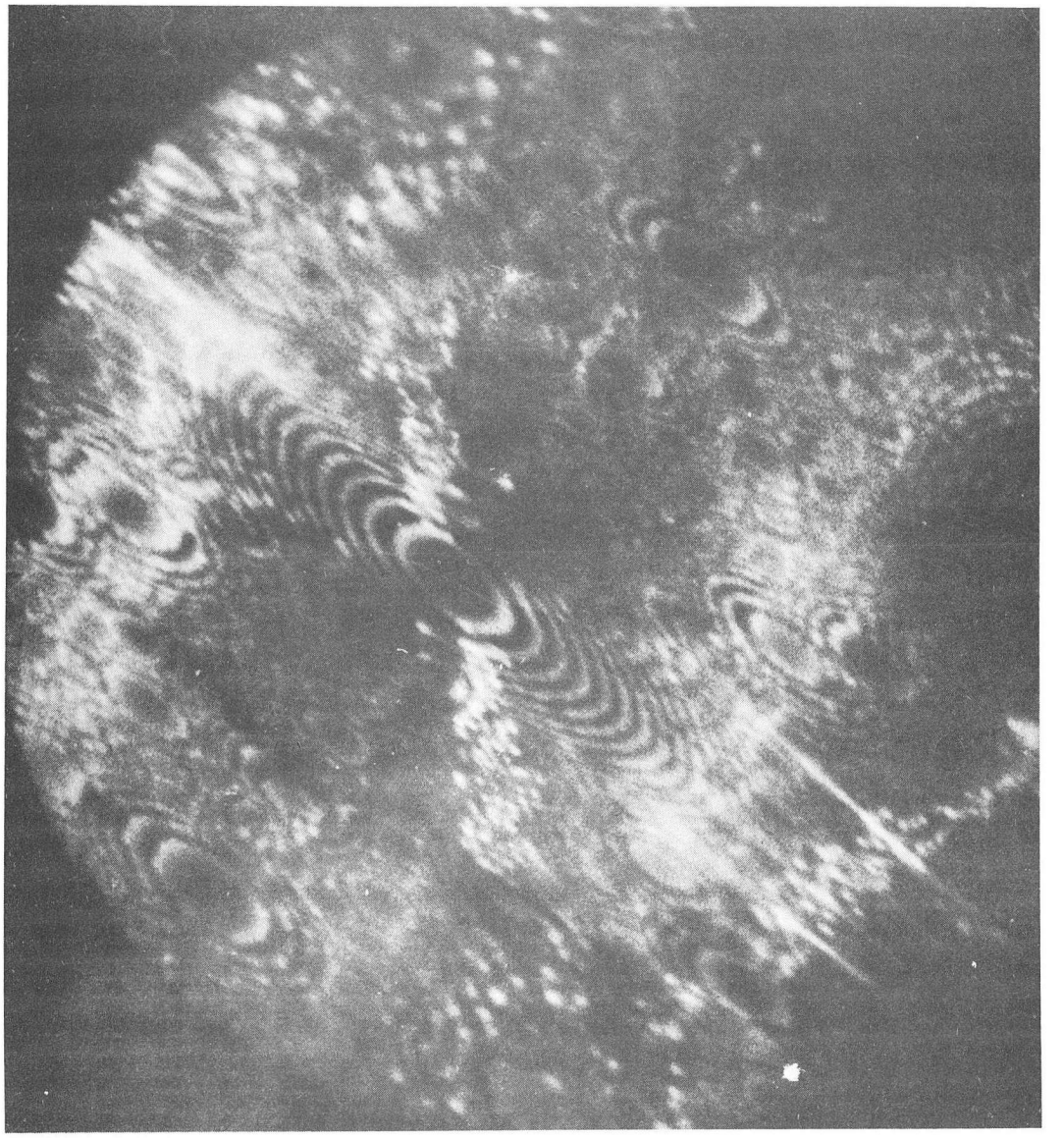

ZN-5392

Fig. 6

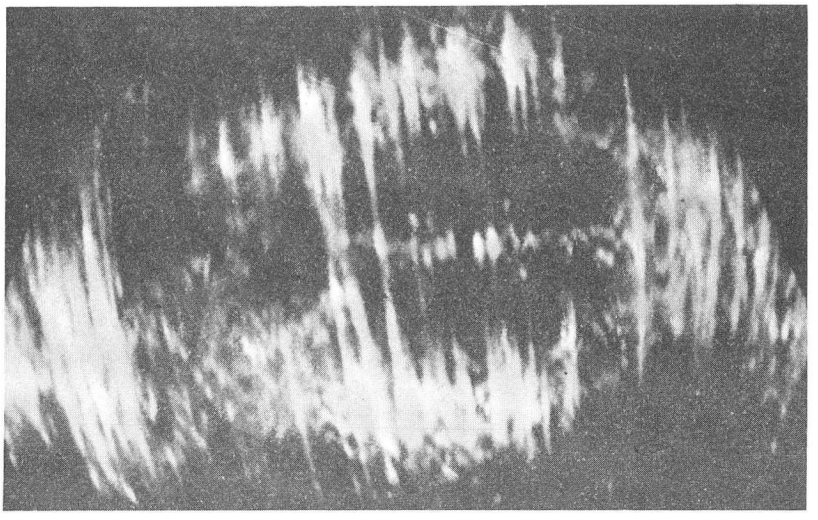

ZN-5396

Fig. 7

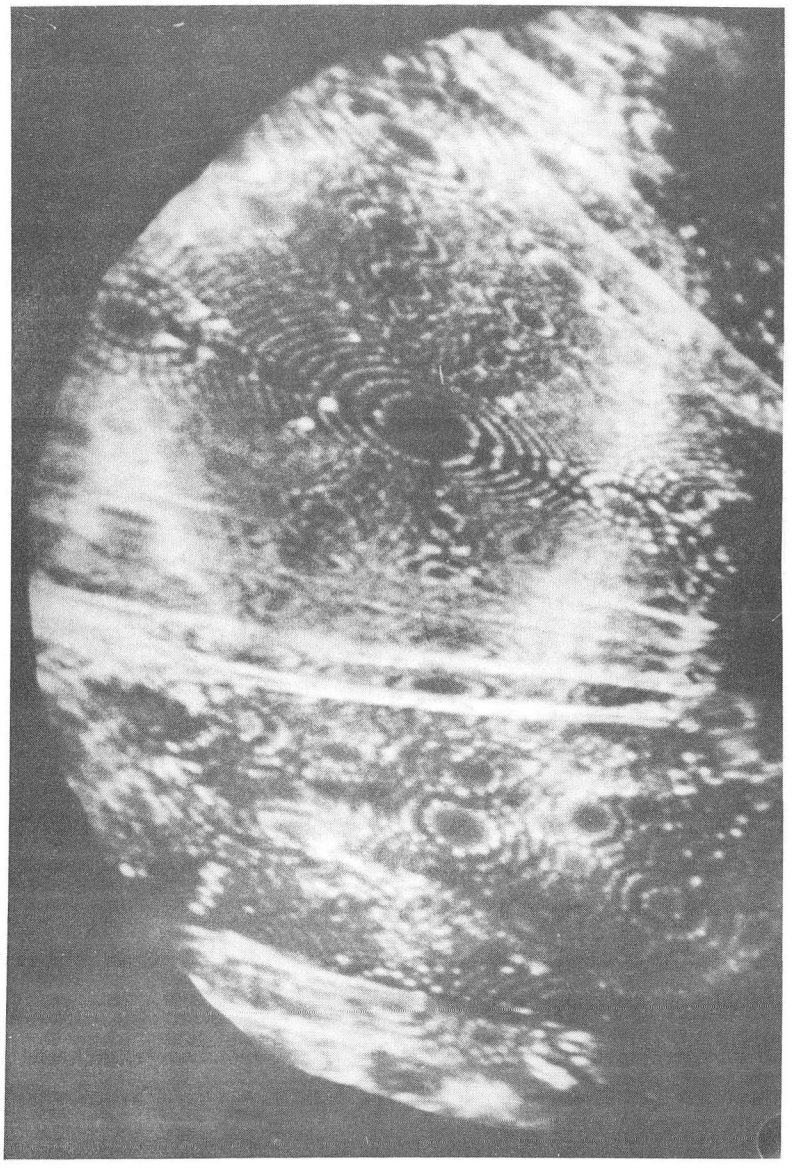

ZN-5393

Fig. 8

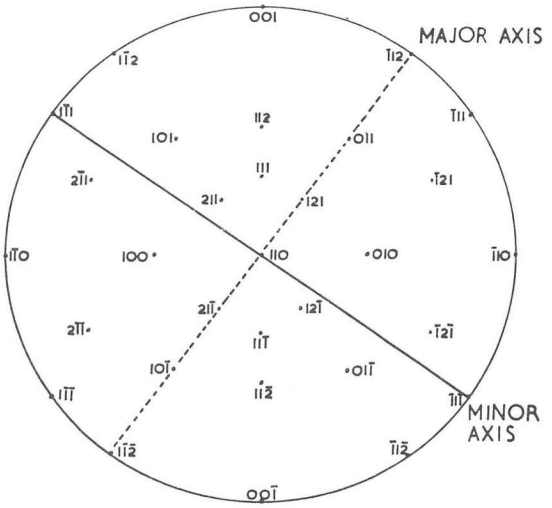

(a)

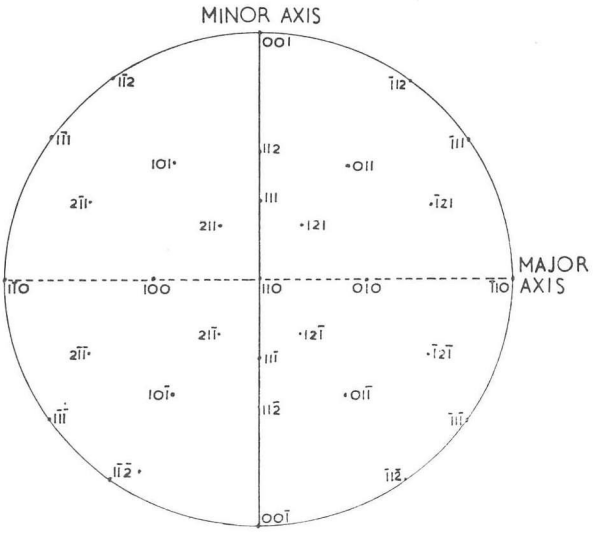

(b)

MUB-9694

Fig. 9

ZN-5397

Fig. 10

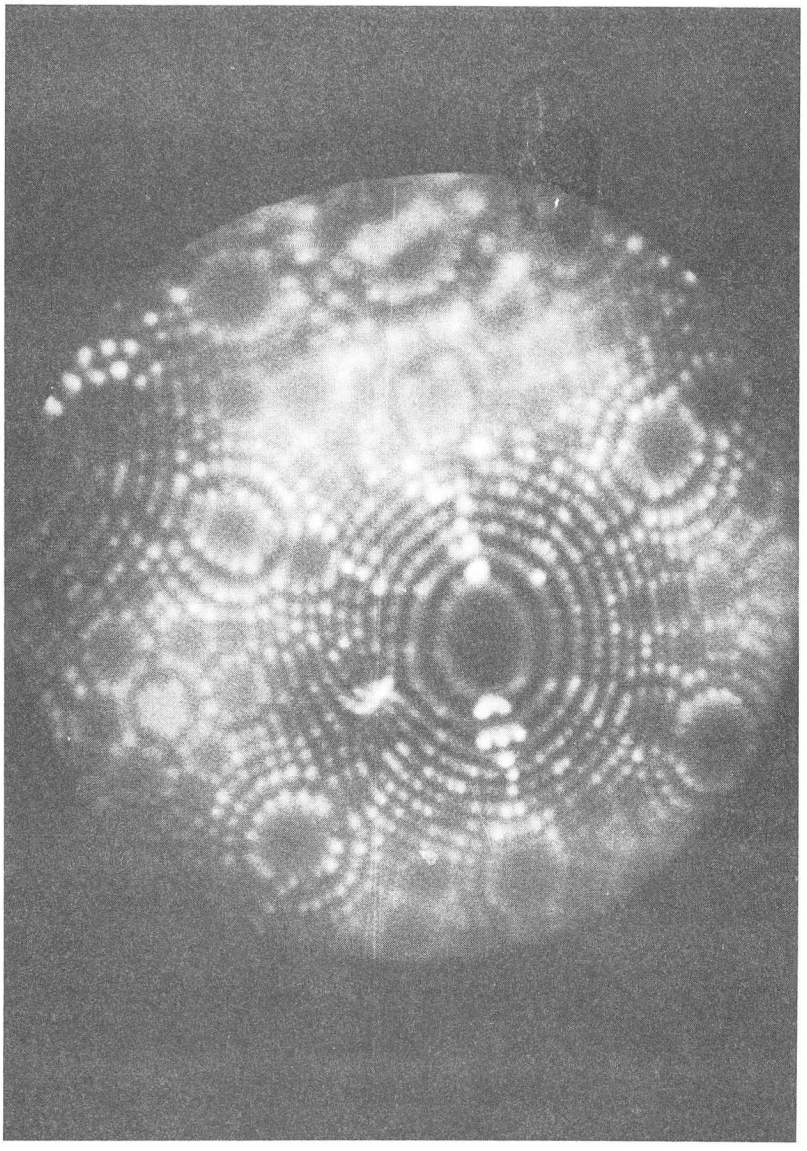

ZN-5391

Fig. 11

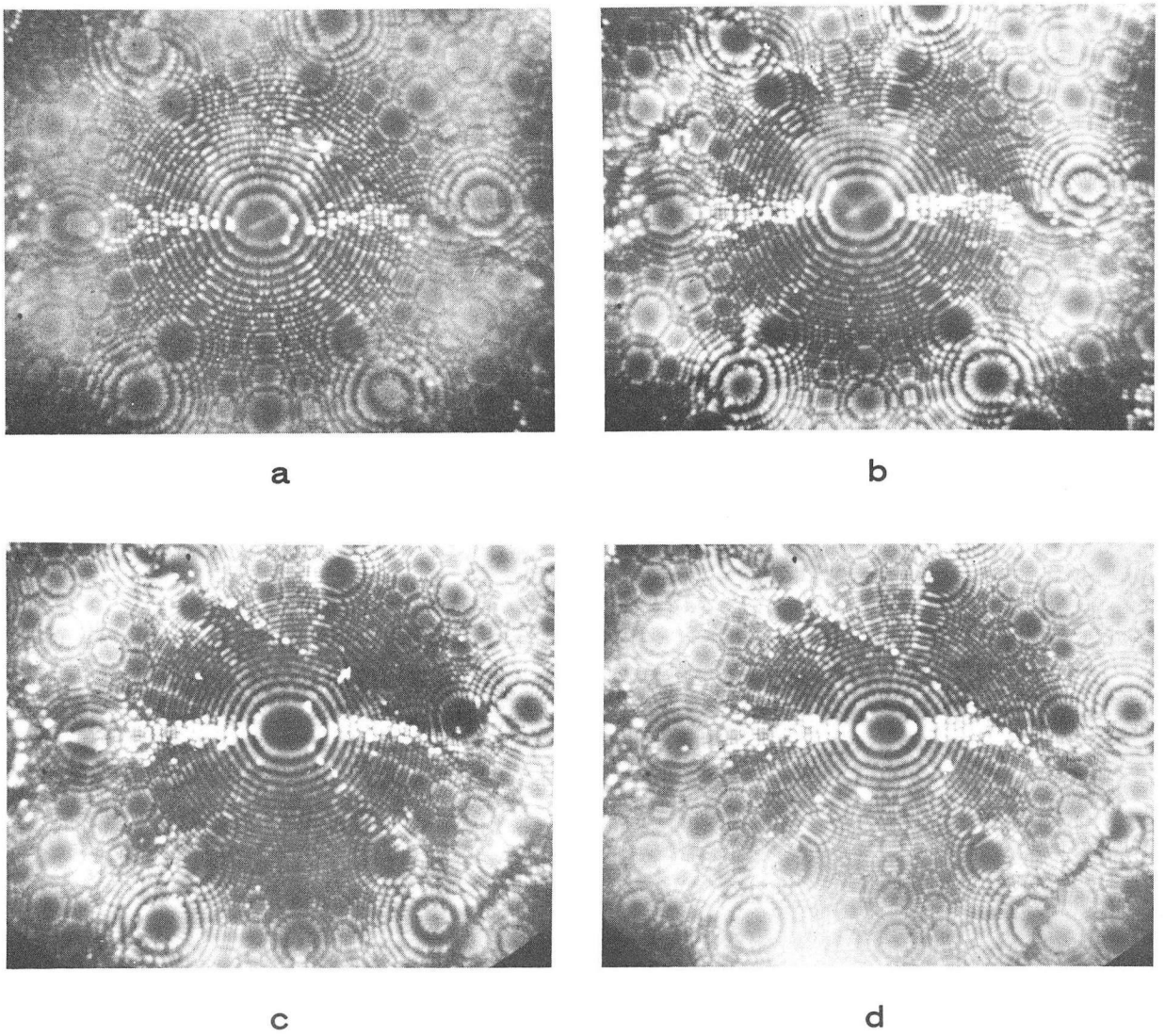

ZN-5394

Fig. 12

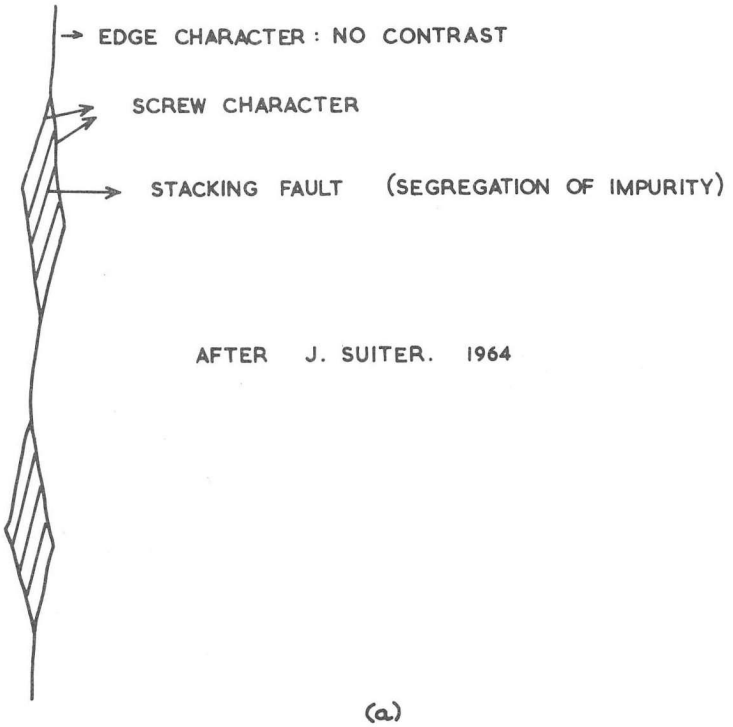

(a)

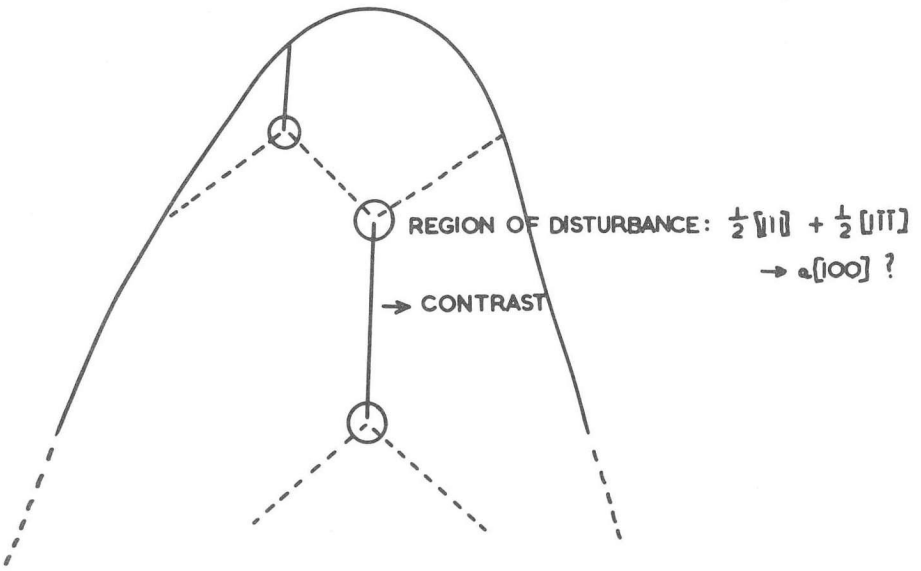

(b)

MUB-9693

Fig. 13

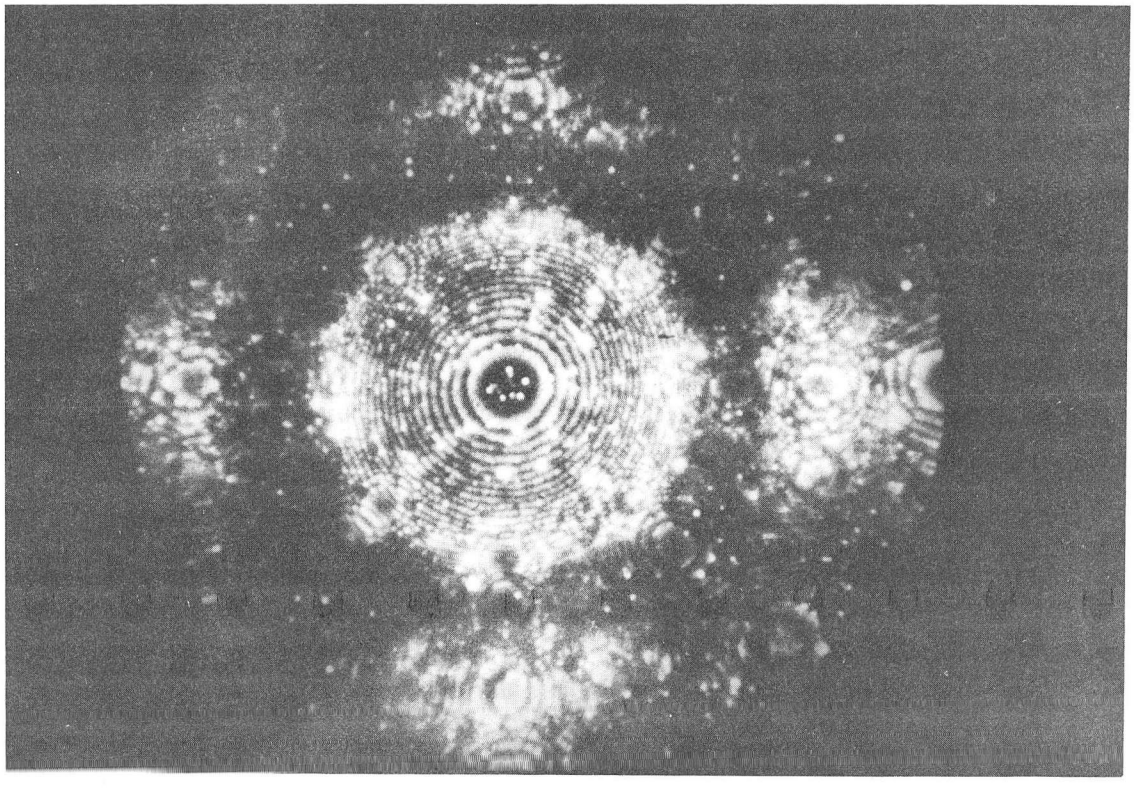

ZN-5289

Fig. 14

This report was prepared as an account of Government sponsored work. Neither the United States, nor the Commission, nor any person acting on behalf of the Commission:

A. Makes any warranty or representation, expressed or implied, with respect to the accuracy, completeness, or usefulness of the information contained in this report, or that the use of any information, apparatus, method, or process disclosed in this report may not infringe privately owned rights; or

B. Assumes any liabilities with respect to the use of, or for damages resulting from the use of any information, apparatus, method, or process disclosed in this report.

As used in the above, "person acting on behalf of the Commission" includes any employee or contractor of the Commission, or employee of such contractor, to the extent that such employee or contractor of the Commission, or employee of such contractor prepares, disseminates, or provides access to, any information pursuant to his employment or contract with the Commission, or his employment with such contractor.